SUPPLEMENTARY INFORMATION

Folding path of P5abc RNA involves direct coupling
of secondary and tertiary structure

Eda Koculi[1,‡] Samuel S. Cho[2,‡], D. Thirumalai[2,*], and Sarah A. Woodson[1,*]
[1]T. C. Jenkins Department of Biophysics, Johns Hopkins University, 3400 N. Charles St., Baltimore, MD 21218 USA and [2]Program in Biophysics, Institute for Physical Sciences and Technology, and Department of Chemistry, University of Maryland, College Park, MD 20742 USA

FIGURE S1
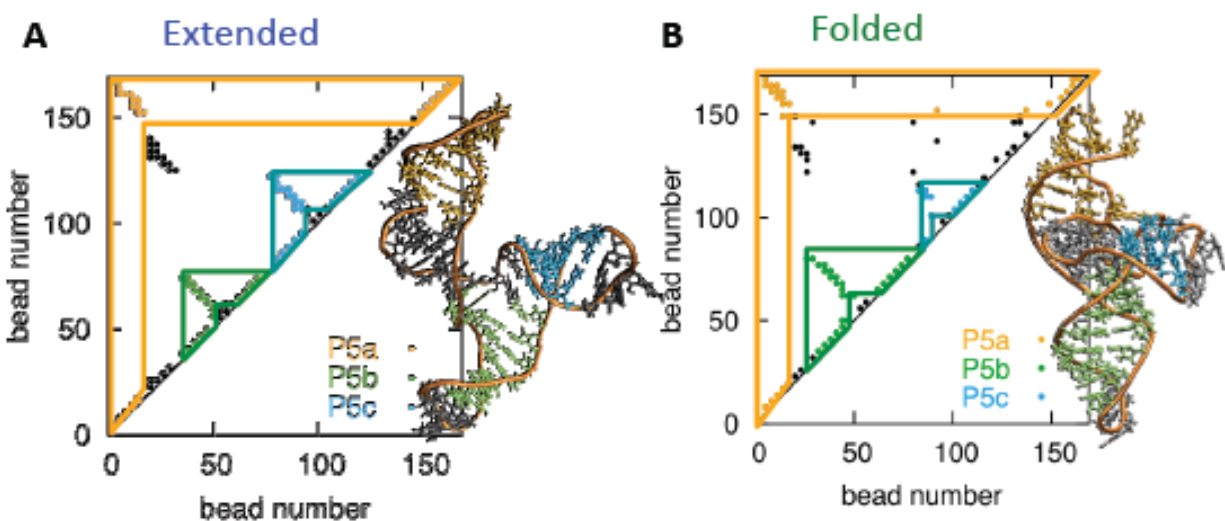
Figure S1. The structure of the extended and folded conformations of tP5abc. A, B. For the extended (A) and folded structures (B), the native interaction map and the corresponding tertiary structures are shown. For the native interaction map, each point represents a pair of bases whose distance is less than 8 Å in the NMR and crystallographic structures of the extended and folded conformations of tP5abc, respectively.

FIGURE S2
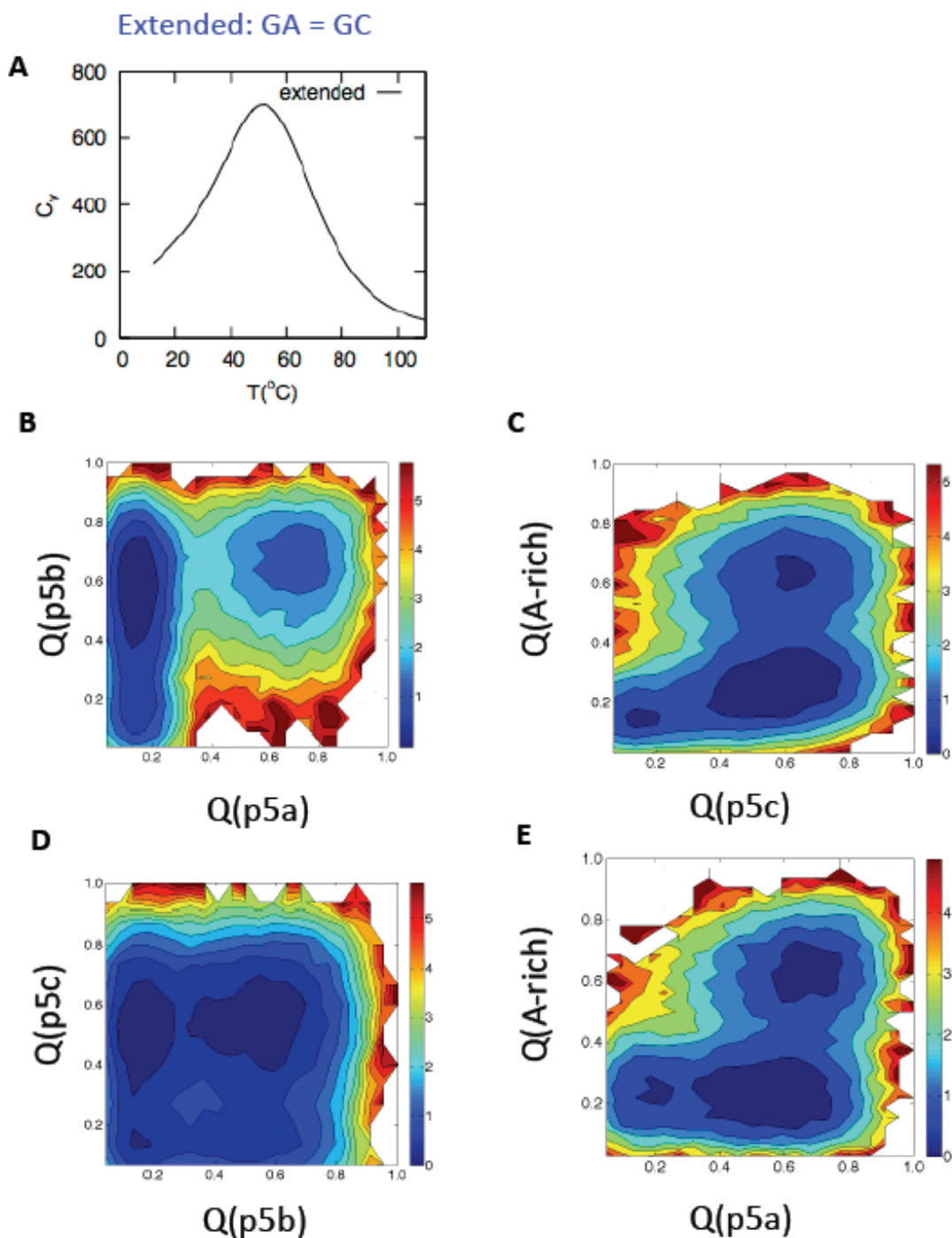
Figure S2. **Comparison of free energy landscapes with G-A and G-C pairs.** Since the stacking interaction energies of the G-A base pairs are not known, those energies were assigned to be the same as if they were G-C pairs, which would be expected to be the upper limit. **A.** Specific heat profile with respect to temperature. **B-F.** Free energy profiles projected to the fraction of native contacts (Q) of various parts of tP5abc.
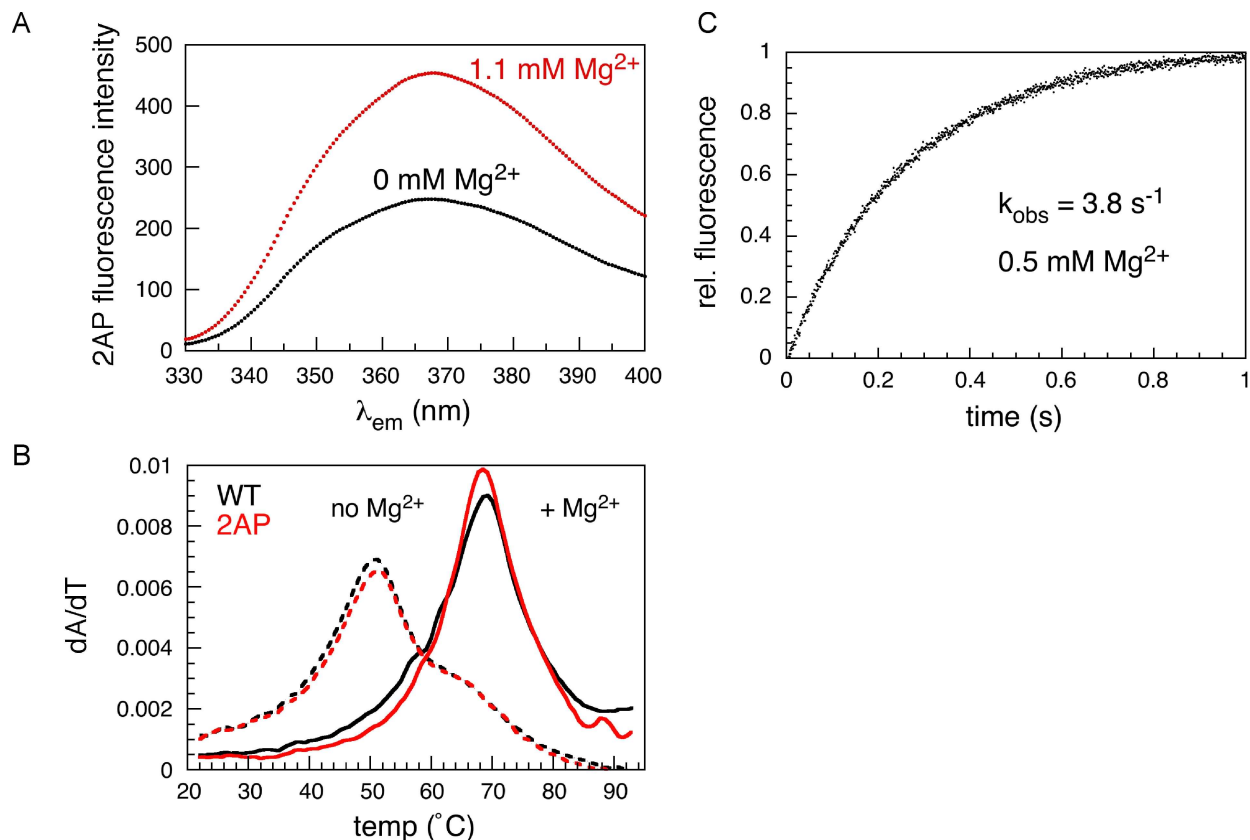
Figure S3. Fluorescence folding assay. A. Emission spectrum of tP5abc-2AP, excited at 310 nm. The 2-aminopurine (2AP) base analog at position 185 unstacks when the RNA folds in Mg^{2+} (red) and the fluorescence intensity increases. **B.** Thermal melting of unmodified tP5abc and 2AP-substituted RNA. Dashed line, no $MgCl_2$; solid line, 2.5 mM $MgCl_2$. Black, unmodified "wild type" tP5abc; red, 2AP modified tP5abc. The first derivative of the absorbance at 260 nm with respect to temperature was fit to two transitions, which were nearly identical in the two RNAs. See Table S1 for fit parameters. **C.** Stopped-flow fluorescence of the folding reaction at 30°C in 0.5 mM $MgCl_2$ (final). The data were fit by a single exponential rate equation.

FIGURE S4
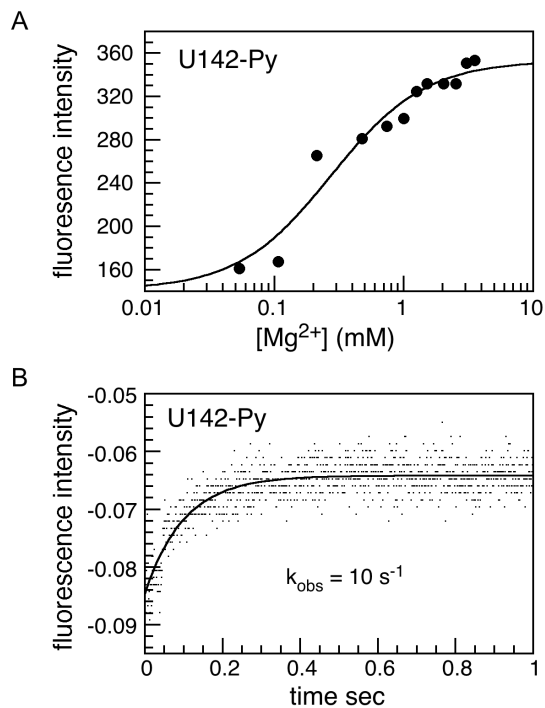
Figure S4. Folding of pyrene-labeled P5abc. tP5abc RNA was conjugated to pyrene through the 2' OH of U142. **A.** Mg^{2+}-dependence of folding in CE buffer. The relative change in fluorescence was fit to the Hill equation, with $C_m \approx 0.28$ mM, compared to 0.18 mM for 2AP-P5abc. **B.** Progress curve for refolding in 0.5 mM $MgCl_2$, with an observed rate constant $\sim$6-10 s^{-1}.

FIGURE S5
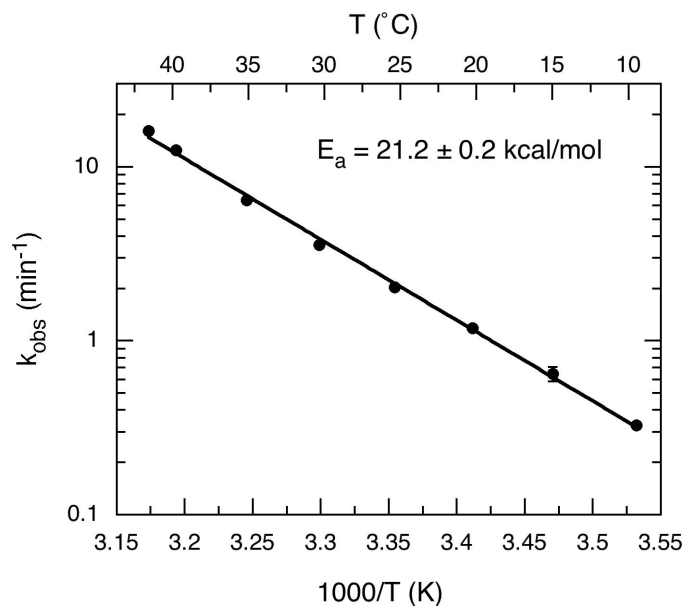
Figure S5. Thermal activation energy of tP5abc folding. Observed folding rates in 0.5 mM Mg^{2+} were measured between 10° and 40°C. Errors are the standard deviation of rate constants from three stopped-flow traces. Data were fit to the Arrhenius equation.

A

$k_{obs} (1) = 2.74 \text{ s}^{-1}$

$k_{obs} (2) = 0.63 \text{ s}^{-1}$

0.5 mM Mg^{2+}

B
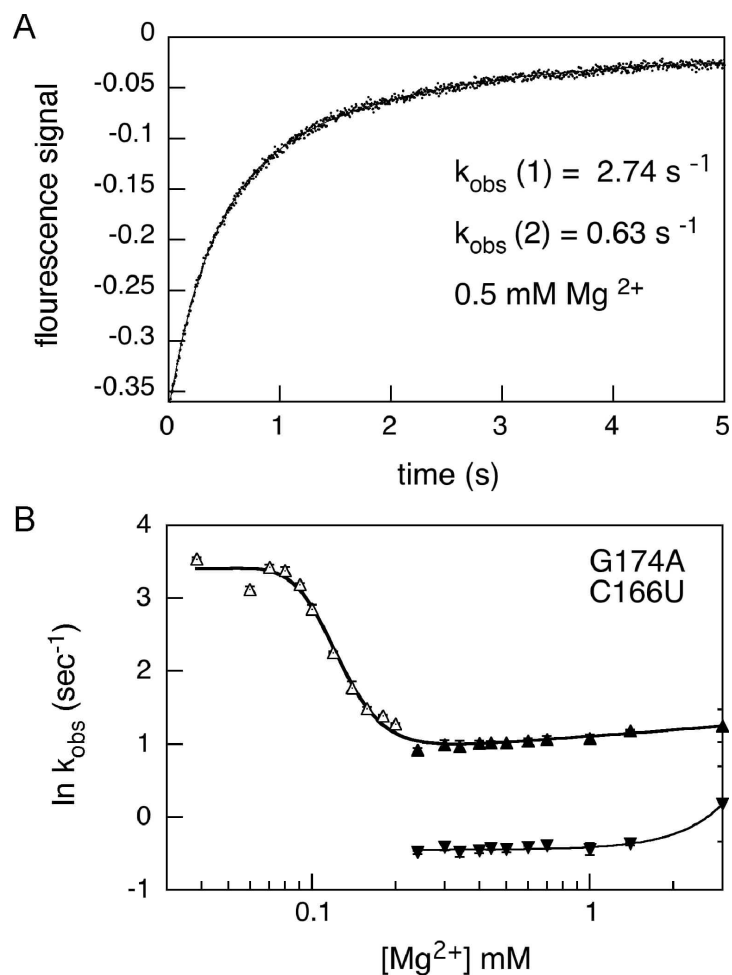
G174A
C166U

Figure S6. Folding of tP5abc:C166U,G174A. Biphasic kinetics were observed for this mutant. **A.** Observed folding kinetics in 0.5 mM MgCl$_2$. The relative amplitude of the slow phase was 15%. **B.** Mg^{2+}-dependence of folding kinetics, showing that neither the fast nor the slow time constant increases with Mg^{2+}. Data fit as in Fig. 7.

Table S1. Thermal stability of tP5abc RNA.

tP5abc	T_{m1} (˚C)	T_{m2} (˚C)	ΔH_1 (kcal/mol)	ΔH_2 (kcal/mol)
no Mg²⁺:				
Wild type	50.5	67.5	48.5	64.0
U185 2AP	50.9	67.5	49.2	70.6
A186U	49.9	55.7	46.8	55.6
+2.5 mM Mg²⁺:				
Wild type	58.7	69.2	38.6	62
U185 2AP	59.1	68.7	35.9	59.9
A186U	66.9	67.6	23.9	37.6

Thermal denaturation was performed in 10 mM Na-cacodylate and 40 mM NaCl. The temperatures and enthalpies of unfolding transitions were obtained using Global Melt Fit as described in Methods.

Table S2. Mg²⁺-dependence of tP5abc folding.

P5abc	C_m (mM) [a]	n_H [a]	ΔG_{UN} (kcal/mol)[b]
Wild type	0.18 ± 0.01	2.7 ± 0.2	-1.3 ± 0.5
+ 60 mM NaCl	1.8 ± 0.3	1.8 ± 0.4	- 0.8 ± 0.2
U168C	0.19 ± 0.02	3.4 ± 0.2	-1.9 ± 0.4
A173G	0.19 ± 0.01	3.2 ± 0.1	-1.9 ± 0.2
G174A,C166U	0.21 ± 0.01	3.1 ± 0.1	-1.9 ± 0.1

[a] Midpoints (C_m) and Hill constants (n_H) were obtained from the fits of 2-aminopurine fluorescence intensity at 370 nm versus Mg²⁺ to the Hill equation at 30 ˚C. The error is the deviation between two independent data sets. [b] ΔG_{UN} was calculated from the cooperativity of the folding transition around the midpoint (Materials and Methods), and is thus more sensitive to the slope of the transition than the midpoint. The error is the deviation between two independent trials.

Table S3. Folding kinetics of tP5abc and transition state structure.

P5abc	k_U (s⁻¹) [a]	k_F (s⁻¹) [b]	$n_U^{\ddagger}$ [c]	$n_F^{\ddagger}$ [c]	β_U [d]	β_F [d]
Wild type	28 ± 1	4.1 ± 0.1	-1.9	0.1	0.7	0.04
+ 60 mM NaCl	16.5 ± 0.3	4.4 ± 0.06	-0.7	0.04	0.4	0.02
U168C	21.7 ± 0.6	3.4 ± 0.02	-3.1	0.2	0.9	0.06
A173G	29 ± 1.7	3.1 ± 0.04	-3.2	0.1	1	0.03
[e]G174A, C166U	29 ± 1.3	3.0 ± 0.2	-2.7	0.1	0.9	0.04

[a]Unfolding rate constant in 0.08 mM $MgCl_2$, or 0.23 mM $MgCl_2$ plus 60 mM NaCl, at 30 ˚C. [b]Folding rate constant in 1 mM $MgCl_2$ or 5 mM $MgCl_2$ plus 60 mM NaCl. Errors are the standard deviation for at least three independent stopped flow traces. [c] $n^{\ddagger}_U$ is the slope of $\ln(k_{obs})$

versus ln [Mg^{2+}] for the unfolding arm of the chevron plot (low Mg^{2+}); n$^{\ddagger}_N$ is the slope for the folding arm of the chevron plot (high Mg^{2+}). The errors in n$^{\ddagger}_U$ and n$^{\ddagger}_N$ from the fit are about ± 20%. [d]Calculated from $\beta_U = n_U^{\ddagger} / n_H$ and $\beta_F = n_F^{\ddagger} / n_H$, respectively. [e]Folding of P5abc:G174A C166U is biphasic; the dependence of the faster phase on Mg^{2+} was used to calculate β_F. For the slower phase, $k_{F,2} = 0.64$ s^{-1} and the amplitude was 15%.